

Time-resolved simultaneous measurement of group index and physical thickness during photopolymerization of resin-based dental composite

Peter H. Tomlins

National Physical Laboratory
Photonics Group
Hampton Road, Teddington
Middlesex TW11 0LW
United Kingdom
and
Cranfield University
Cranfield Health
Bedfordshire, United Kingdom
E-mail: pete.tomlins@npl.co.uk

Will M. Palin

Adrian C. Shortall

The University of Birmingham
School of Dentistry
Saint Chads Queensway
Birmingham B4 6NN
United Kingdom

Ruikang K. Wang

Oregon Health and Science University
Department of Biomedical Engineering
3303 Southwest Bond Avenue
Portland, Oregon 97239
and
Cranfield University
Cranfield Health
Bedfordshire, United Kingdom

1 Introduction

Resin-based composite (RBC) restorative materials have been used in dental practice since the 1960s. Over the years much has been learned regarding the mechanical, physical, and aesthetic requirements of such materials for restorative dentistry. RBCs are increasingly replacing amalgam due to environmental concerns and alleged adverse health effects regarding mercury.^{1,2} However, most studies highlight the decreased clinical longevity of RBCs compared with amalgam restorative materials in large posterior cavities.³⁻⁵ Ten years ago, the consensus among dental practitioners and materials scientists restricted posterior RBCs to small restorations, preferably in premolar teeth with little load-bearing function. Advances in adhesive systems, materials, and restorative techniques have combined to generate significantly improved RBC materials. As a consequence, the use of dental amalgam as a restorative is declining and the number of RBC fillings continues to rise, allowing the consensus of a decade ago to be challenged.⁶

However, one of the principal drawbacks of current light-activated RBCs remains the inefficient setting reactions in

Abstract. Light-activated resin-based dental composites are increasingly replacing dental amalgam. However, these materials are limited by inefficient setting reactions as a function of depth that constrain the maximum extent of cure. Insufficient curing can contribute to an overall reduction in biocompatibility of the material. We demonstrate dynamic refractive index measurements of a commercial dental composite throughout cure using spectral domain low coherence interferometry. Our results show a linear relationship between the change in refractive index and polymerization-induced reduction in physical thickness during light-activated curing. This relationship between the optical and physical density demonstrates the potential of this technique as a unique noninvasive tool for measurement of the conversion degree of curing dental composite materials. © 2007 Society of Photo-Optical Instrumentation Engineers. [DOI: 10.1117/1.2709877]

Keywords: low coherence interferometry; resin-based composite; dental materials; refractive index measurement; optical coherence tomography; polymerization.

Paper 06178R received Jul. 2, 2006; revised manuscript received Sep. 6, 2006; accepted for publication Sep. 8, 2006; published online Feb. 23, 2007.

depth that ultimately place a limit on the maximum depth of cure. The presence of inadequately cured material within a restoration may lead to adhesive failure at the tooth-composite interface,⁷ reduced biocompatibility, and an increased risk of pulpal irritation.⁸ These factors contribute to an overall reduction in the clinical longevity of the restoration. To avoid such effects, clinicians must use incremental layers to place large restorations *in vivo*. This is a time-consuming and costly procedure that increases the risk of voids and contamination leading to a greater risk of early failure. Hence, a decreased number of application steps would provide a more cost effective material for use within the health service. Over the last decade, significant advances have been made in understanding and improving the shortcomings of dental RBCs. However, there remain many unanswered questions concerning the light-activated setting reaction, in particular the change in optical properties upon polymerization.

The depth-dependent extent of cure is commonly evaluated indirectly from hardness measurements made at the nonirradiated surface of resin-based composite disks of different thickness. The depth of cure is defined as the level at which the hardness value is equivalent to a specific percentage of the hardness at the irradiated surface. Direct methods of assessing

Address all correspondence to Ruikang K. (Ricky) Wang, Dept. of Biomedical Engineering, Oregon Health & Science University, 3303 SW Bond Ave., Portland, Oregon 97239; Tel: 503-748-1350; Fax: 503-748-7038; E-mail: r.k.wang@bme.ogi.edu

polymerization include Fourier transform infrared spectroscopy (FTIRS), which relates the degree of cure to the percentage conversion of vinyl (C=C) to aliphatic (C—C) stretching vibrations prior to and following polymerization. Unfortunately, it does not offer us any insight into the rate and extent of any crosslinking reactions. Even with a high degree of conversion, a resin composite based on a composite with few crosslinks may be sensitive to the action of plasticizing compounds in the patient's diet.⁹ Also standard hardness testing does not reveal any problem until the sample has been stored in a suitable solvent such as ethanol for some time.

Although these techniques provide an important indication of curing extent, they do not provide direct information concerning the irradiating light. Monitoring light transmission change during curing has been proposed as a method for predicting an appropriate radiation time of any light-activated resin-based composite irrespective of shade or formulation differences.¹⁰ In addition, this method has been used to investigate the relationship between depth of cure and resin-filler particle refractive index mismatch.¹¹ However, the relationship between the extent and quality of the curing light absorbed and the change in optical properties of the sample remains open to investigation.

In the present work we have used low coherence interferometry (LCI)¹² to study the dynamic change in group index and physical thickness of a commercial RBC. Based on LCI, optical coherence tomography (OCT) has been recently developed into a powerful noninvasive optical technique that is commonly used to image through highly scattering biological tissue, including that of the oral cavity.^{13,14} However, the metrological potential of the technique has, until now, not been applied to the characterization of dental composites. Using this technique, we can simultaneously make time-resolved measurements of the group refractive index, optical thickness, and physical thickness of a dental composite sample before, during, and after the curing process, facilitating the optimization of both optical and physical characteristics of the sample.

The technique of acquiring simultaneously the group index and physical thickness of a semitransparent sample by LCI has been previously described in the time domain.¹⁵ Here we have applied the similar technique known as frequency domain LCI,^{16,17} obtaining spatially resolved results from Fourier transformation of spectrally acquired interference fringes. This is advantageous since, using a fast spectrometer, high acquisition rates can be achieved while maintaining a high signal-to-noise ratio (SNR) compared to time domain techniques.¹⁸ These two characteristics are of prime importance in the present study, since a high dynamic range is required to detect backscattered light from the back surface of the scattering RBC sample at multiple frames per second.

Since the light passes through the sample, the refractive index is an average over index contributions from both the filler and the resin. In practice, this means that the change in measured refractive index will relate to the conversion of monomer to polymeric units throughout the specimen bulk, since the contribution from filler particles will remain constant. This is highly pertinent to typical RBC restorations placed clinically rather than relying on surface measurements alone, such as refractometry. However, a consequence of the interferometric measurement is that we measure the group index rather than the conventional phase index.

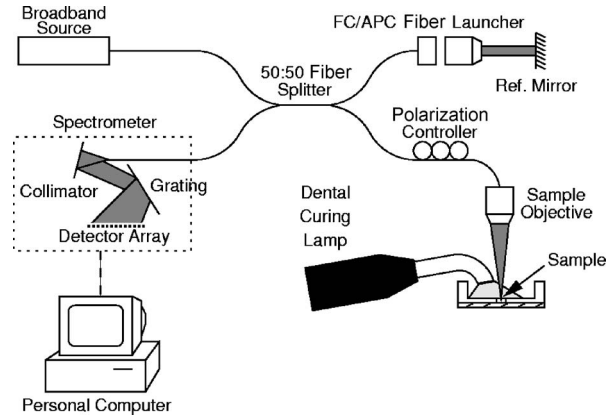


Fig. 1 Experimental arrangement of the frequency domain LCI system used for dynamic thickness and group index measurements of curing dental composite.

2 Theory

Consider a Michelson interferometer configuration such as that shown in Fig. 1, where a broadband input light source illuminates a sample. Backscattered light is coupled back into the interferometer mixing with a reference beam to form interference fringes that are detected at the spectrometer as a periodic intensity modulation in the frequency domain. Fourier transformation of such a spectrogram yields structural information about the sample as a function of optical depth.

If a semitransparent sample is placed in one arm of a Michelson interferometer, butted against a reference backing so that there is no air gap (Fig. 2), it can be shown¹² that the

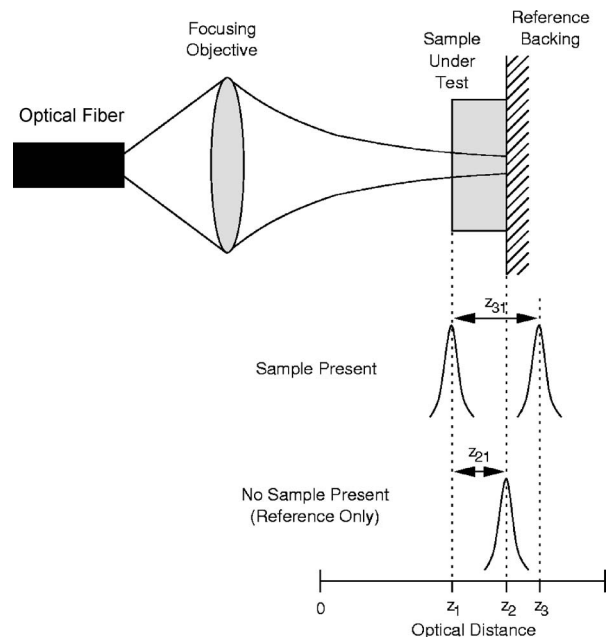


Fig. 2 The sample is placed on a backing surface in one arm of the interferometer. Signals are recorded from the front and back surfaces, z_1 and z_3 , respectively. These are compared with a reference signal from the backing with no sample present z_2 to calculate the group index and physical thickness of the sample.

spectral interference pattern detected at the spectrometer can be computed as

$$I(\omega) = \frac{1}{4}S(\omega)\{1 + \Re[H(\omega)\exp(-i2\omega n_{\text{air}}\Delta z/c)] + |H(\omega)|^2\}, \quad (1)$$

where ω is the optical angular frequency, Δz is the sample and reference arm length mismatch, n_{air} is the refractive index of air, c is the speed of light in a vacuum, and $\Re[\]$ represents the real part of the expression inside the square brackets.

In a highly scattering and therefore lossy media such as RBC, the backscattering intensity is much lower than that in the reference arm. Thus, the last term in Eq. (1), the self-interference term, becomes negligible such that

$$I(\omega) \approx \frac{1}{4}S(\omega)\{1 + \Re[H(\omega)\exp(-i2\omega n_{\text{air}}\Delta z/c)]\}. \quad (2)$$

The sample response function $H(\omega)$ that describes the light propagation through the material can be approximated as follows^{19,20}:

$$H(\omega) = r_f - r_b \exp(-i2\omega nd/c), \quad (3)$$

where d is the physical thickness of the sample and r_f and r_b are arbitrary reflection coefficients that take into account the intensity of the backscattered light corresponding to the front and back interfaces, respectively. The spatial properties of the sample are resolved from the Fourier transform of the detected spectral interference. Therefore, assuming a Gaussian source spectrum of the form

$$S(\omega) = S_0 \exp\left[-\frac{(\omega - \omega_0)^2}{w^2}\right], \quad (4)$$

with center frequency ω_0 and source $1/e$ width $w = \Delta\omega/[2\sqrt{\ln(2)}]$, defined by the full width at half maximum (FWHM) of the source $\Delta\omega$. The envelope of the Fourier transform (FT) of $I(\omega)$ can be determined analytically as

$$\begin{aligned} \text{FT}[I(\omega)] \propto & \exp\left(\frac{-1}{4}w^2t^2\right) + C_f \exp\left[\frac{-1}{4}w^2\frac{(n_{\text{air}}\Delta z - tc)^2}{c^2}\right] \\ & + C_b \exp\left[\frac{-1}{4}w^2\frac{(n_{\text{air}}\Delta z + nd - tc)^2}{c^2}\right]. \end{aligned} \quad (5)$$

The first term in Eq. (5) is the autocorrelation of the source spectrum. The second term is a Gaussian whose peak occurs at an optical distance $z_1 = n_{\text{air}}\Delta z$, and the third term is a Gaussian peak at the optical distance $z_3 = n_{\text{air}}\Delta z + nd$. The arbitrary constants C_f and C_b are related to the front and back reflection coefficients, respectively. When the sample is an optically dispersive medium such as dental RBC, the second peak occurs at a slightly offset location determined by the group index of the material, n_g , i.e., $z_3 = n_{\text{air}}\Delta z + n_g d$, where the group index is defined as²¹

$$n_g(\omega) = n(\omega) + \omega \frac{d}{d\omega}n(\omega). \quad (6)$$

Therefore, the difference $z_{31} = z_3 - z_1$ is the optical group thickness of the sample, also defined as $z_{31} = n_g d$. Hence, if the physical thickness of the sample is known, the group index can also be determined.

Sorin and Gray¹⁵ demonstrated that the physical thickness can be determined by making a similar interferometric measurement of the backing plate position prior to inserting the sample. In this case, the spectrogram is given by

$$I_2(\omega) = \frac{1}{4}S(\omega)(1 + \Re\{\exp[-i2\omega n_{\text{air}}(\Delta z + d)/c]\}), \quad (7)$$

and the corresponding Fourier transform

$$\begin{aligned} \text{FT}[I_2(\omega)] \propto & \exp\left(\frac{-1}{4}w^2t^2\right) \\ & + C \exp\left\{\frac{-1}{4}w^2\frac{[n_{\text{air}}(\Delta z + d) - tc]^2}{c^2}\right\}, \end{aligned} \quad (8)$$

where the second peak is located at $z_2 = n_{\text{air}}(\Delta z + d)$. It therefore follows that the physical thickness of the sample can be obtained using the difference between z_2 and z_1 .

$$z_{21} = z_2 - z_1 \equiv d. \quad (9)$$

Hence, from these two measurements there is sufficient information to recover the group index,

$$n_g = \frac{z_{31}}{z_{21}}. \quad (10)$$

3 Materials and Methods

The configuration of our optical fiber Michelson interferometer arrangement is shown in Fig. 1. The input broadband light source was a superluminescent diode (Superlum SLD-371-MP) with a center wavelength at 830 nm and bandwidth of 49 nm, yielding a spatial resolution of approximately 6 μm in air, from which the interface between layers with an abrupt refractive index change could be located with an accuracy of $<0.1 \mu\text{m}$. An “off the shelf” fiber coupled spectrometer (Ocean Optics HR4000) was used for frequency domain detection leading to a measurement dynamic range of approximately 90 dB. The curing lamp, used to polymerize the RBC samples, was a conventional quartz-tungsten-halogen dental lamp with a nominal wavelength of 470 nm that coincides with the absorption band of the camphorquinone photoinitiator used to initiate the sample curing process. The RBC sample under investigation was Filtek™ Supreme Bodyshade from 3M.

The RBC sample was held in a 2×1 mm hole drilled into the base of a custom-built aluminum holder (Fig. 3) that was designed to fit into a standard 1-in. optical mount. An unpolished metal backing plate was clamped to the back of the sample holder. This served as a reference surface from which the reference signal z_2 was measured. The reference surface was purposely left unpolished, since the diffusely reflected

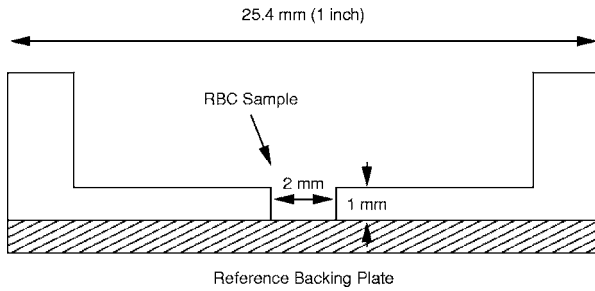


Fig. 3 The sample was held in a 2×1 -mm hole in the base of an aluminum mount. A metal backing plate with a diffuse surface was clamped to the back of the holder to provide a reference surface. The mount fitted a standard 1-in. optical mount.

light could be strongly detected at multiple angles, making the system less sensitive to optical misalignment caused by refraction upon introduction of the RBC sample.

Before introduction of the RBC to the holder, the reference arm of the interferometer was aligned to a position beyond the reference backing plate. In doing this, the signal due to the back surface of the sample is defined with much better SNR and degraded less due to the effect of aliasing during the signal sampling. It is important to optimize for the back surface signal, since it is highly attenuated by the scattering RBC compared to the diffuse reflection from the front surface. To further optimize this signal, the objective was focused onto the reference backing plate.

With the system aligned, a reference measurement was made from the backing plate with no sample present. A series of 100 measurements were made to evaluate the phase stability of the system. These measurements showed the holder position to be stable to within 60 nm over the measurement time.

The sample was pressed firmly into the holder, ensuring that it adhered to the backing plate. Excess RBC was removed from the top of the holder with a scalpel blade to form a small disk of RBC having a diameter of approximately 2 mm and thickness 1 mm.

We acquired spectral data continuously over a 120-s period for six disks of the RBC. The first 40 s were precure and enabled us to establish the baseline variations in the RBC measurement. Following the precure, the sample was illuminated with the dental lamp for 20 s, followed by a post-cure period of 60 s with no illumination. The illumination intensity was approximately 200 mWcm^{-2} .

A computer program was implemented in the SciLab technical computing language to automate the processing of the spectral data. The data were transformed into the time domain and a simple peak tracking algorithm developed to follow the movement of each peak, fitting a Gaussian to precisely determine the location at each point in time. Best results were obtained by averaging sets of ten scans in the time domain. Figure 4 shows the mean average of ten depth resolved measurements from a cured RBC sample. Each depth scan is obtained by Fourier transform of the spectral LCI signal, yielding peaks corresponding to the front and back surfaces, and a smaller signal that is due to light backscattered from filler particles. A set size of ten scans covered a measurement period of approximately 0.5 s, and therefore, such time averaging

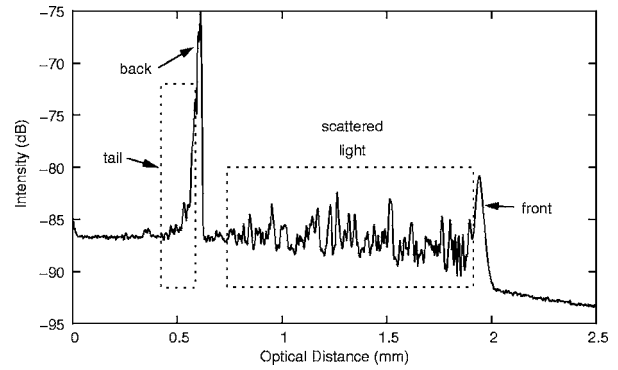


Fig. 4 A typical depth-resolved measurement of the dental composite post-cure. Peaks corresponding to the front and back surfaces of the material are labeled. A Gaussian function was fitted to these peaks to accurately determine their location. The scattered signal is due to the filler particles embedded within the resin, and the tail indicated on the back surface peak is due to multiple scattering. The optical alignment and focus have been optimized for maximum light collection from the back surface of the sample.

ing did not significantly affect the refractive index results, since observed changes occurred slowly over this period. The averaging served to reduce the noise and enhance the small signal from the back of the material.

4 Results and Discussion

Dynamic cure measurements were made on six RBC samples. These resulted in the average refractive index curve shown in Fig. 5. This clearly shows an index change of $\Delta n = 0.0053 \pm 2.5 \times 10^{-5}$ in the sample on photopolymerization. The uncertainty of 2.5×10^{-5} is arrived at from the average of the six refractive index curves, weighted by the variance of a sample of the pre- and post-cure data. The variance of the weighted mean is calculated as $\sigma_n^2 = 1 / (\sum_{i=1}^6 1 / \sigma_i^2)$,^{22,23} where σ_i is the standard deviation of the i 'th curve, i being an integer between 1 and 6. The standard deviation of the pre- and post-cure mean refractive indices are then combined as a sum of squares to calculate the uncertainty of the refractive index difference, which is quoted at one standard deviation. Approximately 90% of the refractive index change occurred over the 20-s curing period, during which the RBC was exposed to the curing lamp, with the remaining 10% change occurring in

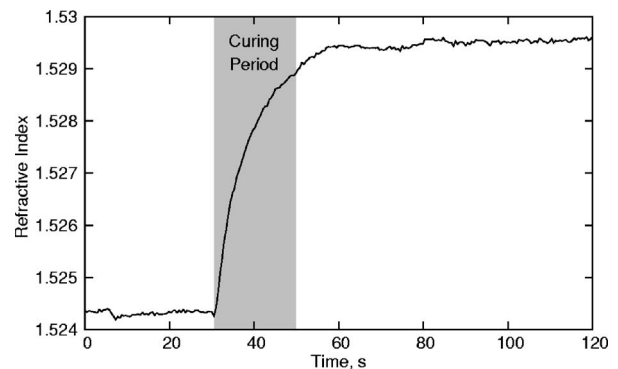


Fig. 5 Time-resolved refractive index curve for curing resin-based dental composite. Average of results for six samples.

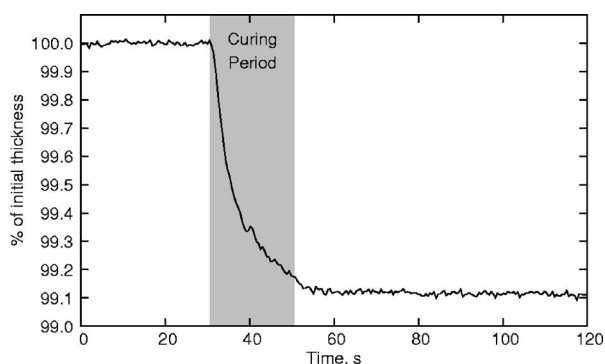


Fig. 6 Time-resolved fractional change in the physical thickness of the dental composite sample during the curing process.

the 5- to 10-s period after irradiation. It is worth noting that while the uncertainty in the index change measurement is relatively small, the absolute group index has a systematic uncertainty of three parts in 10^2 due to variations in the reference surface position between measurements of each sample that occurred as the RBC was introduced into the system. The absolute uncertainty applies equally to all acquired index values that are correlated, and is therefore manifested as a systematic offset to all points in Fig. 5. We have chosen an offset value that matches the cured index value with that obtained for a cured sample using an Abbé refractometer.¹⁹ This falls within the range of the measured values and associated uncertainty. Therefore, neglecting the large systematic uncertainty, the pre- and post-cure refractive index values are $1.5244 \pm 1.4 \times 10^{-5}$ and $1.5292 \pm 2 \times 10^{-5}$. Throughout the measurement of each sample, the reference surface position was stable and was determined to well within two micrometers. The true physical thickness of each uncured sample varied within the range 0.864 to $0.921 \text{ mm} \pm 0.6 \times 10^{-4} \text{ mm}$ between samples, and therefore the thickness changes are presented in Fig. 6 as a fractional change over the measurement period. The thickness change uncertainty is calculated as described before for the refractive index change. It is important to note that while the instrument resolution is only $6 \mu\text{m}$, it is possible to accurately determine the location of a single interface with submicrometer accuracy. The RBC was seen to shrink upon exposure to the curing lamp, with the irradiated surface moving away from the curing lamp. Change to the RBC thickness during curing is a consequence of the free-radical addition polymerization resulting in a net volumetric reduction due to shortening of polymeric chains. The magnitude of thickness change will depend on intrinsic material properties and extrinsic curing parameters, which in turn will affect the refractive index change. This is currently being investigated by the authors using model unfilled and filled resins.

Upon irradiation of the sample, a rise in the RBC refractive index was observed (Fig. 5) as the polymeric system density increased. Simultaneously, as the polymerization degree increased, the physical thickness of the sample decreased (Fig. 6). It can be seen from Fig. 7 that the change in refractive index is inversely proportional to the change in physical thickness. This indicates that the index change is largely due to an increase in the physical density of the RBC, rather than

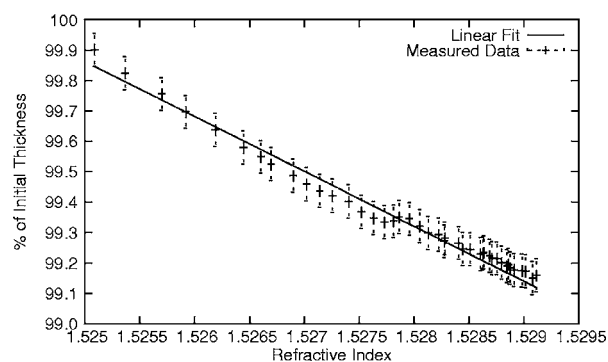


Fig. 7 Linear relationship between the change in physical thickness and refractive index.

any significant change to the fundamental interaction between the optical field and the monomer/polymer molecules. Assuming that the shrinkage is entirely due to polymerization, the linearity of the thickness-index relationship therefore has the potential to provide a measure of the polymerization degree. A small departure from linearity can be seen in the data: however, this is at a level below the uncertainty and is therefore difficult to assess with any quantitative accuracy. The presence of nonlinearity may indicate a more fundamental change to the optical interaction with the RBC material during monomer to polymer conversion. However, the complexity of the optical transmission properties of the curing specimen warrants further investigation, with explicit consideration of the polymerization degree.

It follows that the depth-dependent RBC refractive index is also of interest. A nonuniform refractive index profile throughout the specimen depth is expected to arise due to the decrease in curing light intensity with increasing sample thickness, and hence a reduced monomer to polymer conversion. Therefore, the refractive index profile will relate to the extent of polymerization at corresponding depths. While we believe that it may be possible to calculate the refractive index profile from the LCI data, further studies must be conducted using samples of different thickness to verify these results.

In this work, we used an optical broadband source operating in the 830-nm region, limiting sample thicknesses to $<1 \text{ mm}$ that is of less clinical interest than samples double this size. Probe depth issues could be resolved by using a higher power source in conjunction with a more sensitive detection system, or by working at a longer wavelength that is less scattered by the RBC. However, as the wavelength of the probe is varied, optical dispersion would cause a change in the measured refractive index. It remains to be shown whether this would have a significant effect on the index change: however, differences in the dispersion curves for both the monomer and polymer would lead to either a smaller or larger change. The linearity result described before suggests that the index change is predominantly due to polymerization shrinkage. Therefore, the monomer and polymer dispersion curves may be similar, resulting in no significant wavelength dependence on the refractive index change. Similar measurements to those described in this work could be carried out at two distinct wavebands to test this hypothesis and correlate any differences. Should the refractive index change at longer

wavelengths be larger, then this may be advantageous in providing a greater dynamic range and lower noise. Optimization of the refractive index difference is particularly relevant to future dental materials research. Generally, there are differences where the optimal index change of the RBC is dependent on the desired clinical outcome. To maximize the light transmission and hence depth of cure, it is preferable to match the refractive index of the filler particles with that of the resin. Aesthetics of the final restoration may require a large mismatch between the filler and resin refractive index to produce an opaque material or a smaller mismatch to produce a material that is more translucent, mimicking the optical properties of enamel. In such cases, it is desirable to optimize the refractive index change, so that maximum transmission occurs at the beginning of the curing process, but the final refractive index satisfies the aesthetic requirements. This is yet to be fully resolved and is the subject of current investigations by the authors.

By further phase stabilization of our OCT system, the measurement uncertainties could be reduced to obtain both a more accurate absolute group index measurement but also precise index change and thickness values. Improved intermeasurement stability of the reference backing position will also greatly improve the absolute index measurement and enable small changes in z_3 to be resolved. This is essential for further analysis of the linear dependence of n on d . In the present study, a significant source of uncertainty is in the data analysis itself. When a curve is fitted to each peak to identify its location, noise due to speckle and multiple scattering within the glass filler material leads to extra peaks that can weight the fitted result, or, in some circumstances, fool the fitting routine into minimizing to the wrong peak. Often this effect can be easily identified and corrected by inspection of the processed data. However, in some cases it simply leads to an increased noise and uncertainty in the resultant index or thickness curve. We estimate that this effect can contribute to the back surface uncertainty by up to $\pm 1 \mu\text{m}$. There is a further uncertainty contribution that is due to multiple scattering of the probe light. The so-called ballistic photons are not significantly scattered and therefore travel the shortest path through the RBC specimen. This light forms the main peak that corresponds with the sample back surface. However, some light is scattered multiple times within the material and therefore takes a much longer path before arriving at the detector, leading to a tail that extends the main peak. Such a tail can be clearly seen in Fig. 4 on the peak corresponding to the back surface. This asymmetry can lead to a small error in the Gaussian fit. Analysis of our results suggests that in the present case, this effect can weight the measurement of z_3 by as much as $+1 \mu\text{m}$. However, since the RBC is highly scattering both before and after curing, the effect on the index change measurement is expected to be no more than a part in 10^4 .

5 Conclusions

We demonstrate a novel application of LCI to the simultaneous dynamic measurement of group index and physical thickness of dental RBC. The change in group index and physical thickness are observed before, after, and throughout cure of the dental RBC material. The irradiated surface of the RBC is also seen to shrink away from the curing lamp. Our

results also clearly show the signal corresponding to scattering particles within the RBC. This has implications for the future measurement of refractive index and dispersion throughout the material depth.

Our results show a linear relationship between the physical thickness and refractive index change of the RBC throughout the curing process. This agrees with our hypothesis that the index change should relate to the polymerization degree. The linearity with respect to physical thickness suggests that the index change is due primarily to the polymerization-induced increase in physical density. However, further studies are required with an increased sensitivity, lower uncertainty, and an independent measure of the polymerization degree to verify this conclusion. Measurements of optical dispersion would also provide additional useful information.

This measurement technique provides a new way to study the dynamic behavior of dental materials. Understanding of the dynamic behavior of the RBC refractive index is of fundamental importance to its optimization and use. Light transmission through RBC is also very important, with recent studies being conducted on resins with different monomer blends and filler types,²⁴ providing RBC samples with a wide variation in resin and filler refractive index. Future investigations should be carried out on samples of varying thickness and composition, making dynamic measurements of both light transmission and refractive index change. This will help to understand the index change due to the light absorption.

Acknowledgments

The authors would like to thank Scott Prah and Sean Kirkpatrick of Oregon Health and Science University for helpful discussion. This work was supported by the UK's Department of Trade and Industry's National Measurement System Directorate (NMSD) under contract number GBBK/C/11/12.

References

1. F. J. Burke, "Amalgam to tooth-coloured materials—implications for clinical practice and dental education: governmental restrictions and amalgam-usage survey results," *J. Dent.* **32**, 343–350 (2004).
2. R. E. Bogacki, R. J. Hunt, M. del Aguila, and W. R. Smith, "Survival analysis of posterior restorations using an insurance claims database," *Oper. Dent.* **27**, 488–492 (2002).
3. P. Lucarotti, R. Holder, and F. Burke, "Outcome of direct restorations placed within the general dental services in England and Wales (part 1): Variation by type of restoration and re-intervention," *J. Dent.* **33**, 805–815 (2005).
4. I. A. Mjor, J. E. Dahl, and J. E. Moorhead, "Age of restorations at replacement in permanent teeth in general dental practice," *Acta Odontol. Scand.* **58**, 97–101 (2000).
5. T. Sheldon and E. Treasure, "Dental restoration: what type of filling?" *Effective Health Care* **5**, 1–12 (July 1999).
6. J. Roeters, A. Shortall, and N. Opdam, "Can a single resin composite serve all purposes?" *Br. Dent. J.* **199**, 73–79 (July 2005).
7. W. M. Palin, G. J. Fleming, H. Nathwani, F. J. Burke, and R. C. Randall, "In vitro cuspal deflection and microleakage of maxillary premolars restored with novel low-shrink dental composites," *Dent. Mater.* **21**, 324–335 (2005).
8. A. C. Shortall, H. J. Wilson, and E. Harrington, "Depth of cure of radiation-activated composite restoratives—Influence of shade and opacity," *J. Oral Rehabil.* **22**, 337–342 (1995).
9. E. Asmussen and A. Peutzfeldt, "Influence of pulse-delay curing on softening of polymer structures," *J. Dent. Res.* **80**, 1570–1573 (2001).
10. E. Harrington, H. J. Wilson, and A. C. Shortall, "Light activated restorative materials: a method of determining effective radiation times," *J. Oral Rehabil.* **23**, 210–218 (1996).
11. K. Fujita, N. Nishiyama, K. Nemoto, T. Okada, and T. Ikemi, "Effect

- of base monomer's refractive index on curing depth and polymerization conversion of photo-cured resin composites," *Dent. Mater. J.* **24**(3), 403–408 (2005).
12. P. H. Tomlins and R. K. Wang, "Theory, developments and applications of optical coherence tomography," *J. Phys. D* **38**, 2519–2535 (2005).
 13. B. W. Colston Jr., M. J. Everett, L. B. Da Silva, L. L. Otis, P. Stroeve, and H. Nathel, "Imaging of hard- and soft-tissue structure in the oral cavity by optical coherence tomography," *Appl. Opt.* **37**, 3582–3585 (1998).
 14. L. L. Otis, B. W. Colston Jr., M. J. Everett, and H. Nathel, "Dental optical coherence tomography: a comparison of two in vitro systems," *Dentomaxillofac Radiol.* **29**, 85–89 (2000).
 15. W. V. Sorin and D. F. Gray, "Simultaneous thickness and group index measurement using optical low-coherence reflectometry," *IEEE Photonics Technol. Lett.* **4**, 105–107 (1992).
 16. V. N. Kumar and D. N. Rao, "Using interference in the frequency domain for precise determination of thickness and refractive indices of normal dispersive materials," *J. Opt. Soc. Am. B* **12**, 1559–1563 (1995).
 17. A. F. Fercher, C. K. Hitzenberger, G. Kamp, and S. Y. El-Zaiat, "Measurement of intraocular distances by backscattering spectral interferometry," *Opt. Commun.* **117**, 43–48 (1995).
 18. R. Leitgeb, C. Hitzenberger, and A. Fercher, "Performance of Fourier domain vs. time domain optical coherence tomography," *Opt. Express* **11**, 889–894 (2003).
 19. P. H. Tomlins and R. K. Wang, "Matrix approach to quantitative refractive index analysis by fourier domain optical coherence tomography," *J. Opt. Soc. Am. A* **23**, 1897–1907 (2006).
 20. P. H. Tomlins and R. K. Wang, "Simultaneous analysis of refractive index and physical thickness by fourier domain optical coherence tomography," *IET Proc. Optoelec.* **153**, 222–228 (2006).
 21. G. P. Agrawal, *Nonlinear Fiber Optics*, 2nd ed., Academic Press, New York (1995).
 22. P. R. Bevington and D. K. Robinson, *Data Reduction and Error Analysis for The Physical Sciences*, McGraw-Hill, New York (2003).
 23. N. F. Zhang, "The uncertainty associated with the weighted mean of measurement data," *Metrologia* **43**, 195–204 (2006).
 24. A. Ogunyinka, W. M. Palin, A. C. Shortall, and P. M. Marquis, "Photoinitiation chemistry affects light transmission and degree of conversion of curing experimental dental resin composites," *Dent. Mater.* **2006**, preprint (2006).